Does shape matter? FEMDEM estimations of strength and post failure behaviour of catalyst supports

A. Farsi[1], J. Xiang[1], J. P. Latham[1], M. Carlsson[2], E. H. Stitt[2], M. Marigo[2]

[1]Applied Modelling and Computation Group (AMCG),
Department of Earth Science and Engineering
Imperial College London, South Kensington Campus,
London SW7 2AZ, United Kingdom

[2]Johnson Matthey, P.O. Box 1, Belasis Avenue,
Billingham, Cleveland, TS23 1LB, United Kingdom

ABSTRACT

The combined finite-discrete element method (FEMDEM) implemented in Solidity is employed to simulate the effects of geometrical features and loading orientation on the pre- and post-failure behaviour of catalyst supports. In this paper, a comparison with experimental results and a mesh sensitivity analysis for the numerical simulations of uniaxial compression tests on cylindrical pellets are presented and discussed. The structural strength of complex-shaped pellets under simplified loading conditions is investigated with numerical simulations. Some preliminary results that give an insight into the relation between the shape of catalyst supports and their mechanical performance are also presented and discussed.

1 Introduction

The catalysts typically employed for fixed-bed reactors in steam reformers contain an active metal component supported on porous materials with a high surface area, most commonly alumina (aluminium oxide, Al_2O_3). To maximise the available surface area and increase heat transfer, these supports can be shaped as cylindrical pellets, balls or more complex configurations. In conventional reforming processes, reaction temperatures in the 450-950 °C range are required depending on the application [1]. For this reason the bundles of tubes are suspended in a heated chamber, as shown in Figure 1.

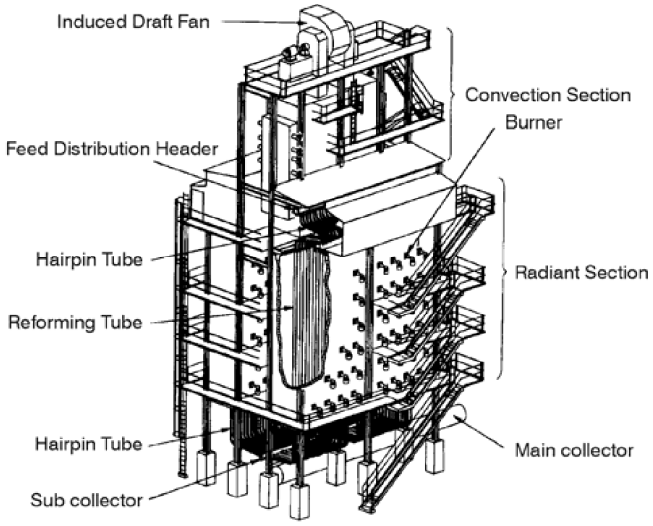

Figure 1: Topsoe reformer with burners placed on side walls [1].

A better understanding of fracture propagation in packed structures of ceramic bodies is crucial to the development of new strategies to reduce the accumulation of catalyst fragments and to extend the lifetime of reactors, and further innovations in fixed-bed reactor technology.

In this work, the effects of the catalyst support shapes on their final strength and fragmentation behaviour are investigated through controlled experiments and numerical simulations. Uniaxial compression tests and high-speed video recordings are employed to estimate strengths and pellet crushing behaviours. The combined finite-discrete element method (FEMDEM) implemented in Solidity [2] is employed to simulate the effects of geometrical features and loading orientation on the pre- and post-failure behaviour of catalyst supports. In this paper, a comparison with experimental results and a mesh sensitivity analysis for the numerical simulations of uniaxial compression tests on cylindrical pellets are presented and discussed. The structural strength of complex-shaped pellets under simplified loading conditions is investigated with numerical simulations and some preliminary results are also presented and discussed.

2 Uniaxial compression

The uniaxial compression test apparatus was mounted an actuators to apply a uniaxial load, as described in [3]. The loading plates and the tested samples have been modelled with 2D Solidity FEMDEM simulations. Both tests and simulations have been performed on discs with and without holes. In this work, two sets of specimens (Set 1 and 2) with different diameters (D), holes diameters (d), thicknesses (t) and mechanical properties have been considered. The geometries are summarised in Table 1.

Table 1: Average of the measured dimensions and bulk density of the tested specimens.

Set		D [mm]	d [mm]	t [mm]	Bulk density [g/cm^3]
1	Disc	18.56 ± 0.01	-	19.16 ± 0.01	2.32
	4-hole	18.39 ± 0.01	5.14 ± 0.01	12.54 ± 0.01	2.31
2	Disc	17.69 ± 0.01	-	18.36 ± 0.01	2.69
	4-hole	17.56 ± 0.01	4.88 ± 0.01	12.00 ± 0.01	2.64

The mesh and boundary conditions are shown in Figure 2(a) and 4(a), 4(c) respectively. The experiments were also recorded with a high-speed camera to determine the fracture paths and pellet crushing behaviours. In the numerical simulations, the bottom plate is fixed and the top loading plate is constrained with constant velocity. The velocity of the constraint is set to 0.01 m/s, which is the loading rate that was set in the laboratory experiments. To reduce the calculation time, when the simulation starts, the top plate is in contact with the specimen and for this reason an initial velocity equal to the one applied to the constraint is imposed on the loading plate. The specimen is discretised with an unstructured fine mesh to better represent both the de-bonding stress during the opening of the cracks and the fracture path along the element boundaries. The total number of elements employed in the simulations of discs with and without holes is about 37,000 and 53,000 respectively. The material properties used to describe the loading plates are E_s=210 GPa, ν_s=0.3 and ρ_s=7850 kg/m^2, where E_s is the Young's modulus, ν_s is the Poisson's ratio and ρ_s is the density. The material properties used for the specimens vary depending on the bulk density of the tested sample. Figure 2 shows the simulation results of a disc with no holes from Set 1, with E_c=40.05 GPa, ν_c=0.17, ρ_c=2310 kg/m^2, f_t=5.07 MPa and G_I=0.2 J/m^2. Since a value of fracture toughness was not available for the cylindrical samples, values G_I have been optimised for the sets of sample to obtain the correct failure mechanism for the uniaxial compression of a disc. In other words G_I

has been selected from the simulation showing a fracture initiating from the centre of the disc and propagating to the two contact points. The same values of energy release rate have been used for the simulations of uniaxial compression of pellets with four holes with the same bulk density. Figure 5 compares of the simulation results for discs with four holes from Set 1, with the corresponding results for samples from Set 2 with E_c=50.08 GPa, ν_c=0.17, ρ_c=2690 kg/m^2, f_t=10.62 MPa and G_I=0.4 J/m^2.

3 Results and discussion

Figure 2(b) shows the horizontal stresses reaching the value of tensile stress (red) in the centre of the disc before failure. After that point, a fracture initiates from the centre and propagates diametrically to the two points of contacts, as shown in Figure 2(c). While the fracture reaches the two points of contact, also the applied load drastically decreases and the two halves of the disc fragment under the action of the two loading plates as shown in Figure 2(d). The simulation results can be compared with two frames obtained from the high-speed video recordings of the test of a disc with no holes from Set 1 shown in Figure 2(e) and 2(f). Assuming an elastic response of the disc to a linearly increasing load, and that the applied load is transmitted by each loading plate on a flat 200 μm portion of the disc surface (i.e. an angle $\alpha = 0.6°$ between the centre of the loading plate, the centre of the disc and the extreme point of the contact surface between the disc and the plate), an approximate solution for the relation between the plate displacement (d) and applied load during the test (P) can be defined in equation (1) [4].

$$d = -\frac{2P}{\pi\ E\ t}[(1-\mu) - log(1+\frac{4}{sin^2(\alpha)})]\frac{\alpha}{sin(\alpha)} \tag{1}$$

In Figure 3 the load-displacement curve calculated in the numerical simulation is compared with the approximated experimental curve calculated with equation (1). The maximum value for the contact force is slightly higher in the numerical results than in the theoretical prediction. This could be because the mesh elements are not all perfectly aligned across the vertical plane where the stress field develops its maximum tension.

Numerical simulations of the uniaxial compression tests on the disc with four holes have been carried out loading specimens with different orientations, i.e. with respect to the angles between the line of the contact points and the symmetry axes of the discs created by the four hole locations. When the two hole centres lie directly in line with the loading points, this is called the 'weak orientation'. Whereas, when the two hole centres lie perpendicularly to line with the loading points, this is called the 'strong orientation'. Loading orientations at intervals of 5° have been considered between the weak (0°) and the strong (45°) orientation configuration of the four-hole disc. Figure 4 shows the loading conditions and load-displacement curves obtained from uniaxial compressive test simulations on the four-hole specimens from Set 1. The load that makes the first fracture initiating within the pellet (i.e. when the first joint element in the FEMDEM discretisation breaks [5]) is determined by inspecting the fracture walls in the numerical results. In Figure 5 the load at failure calculated in the numerical simulation for the different orientations of pellets with four holes from Set 1 and 2 is compared. The values of load have been normalised with respect to the strength of an equivalent cylinder of identical geometry and mechanical properties without holes. This normalisation allows to clearly visualise and compare the interaction of internal geometrical features and loading orientations on samples with different sizes and mechanical properties. This would have been otherwise impossible as the failure loads may differ of orders of magnitude. Figure 5 shows a good agreement between the two normalised curves, demonstrating a similar trend of the structural strengths for the two sets of samples. Figure 5 shows also that the structural strength of pellets that are loaded on their strong orientations is consistently almost five times greater than the structural strength

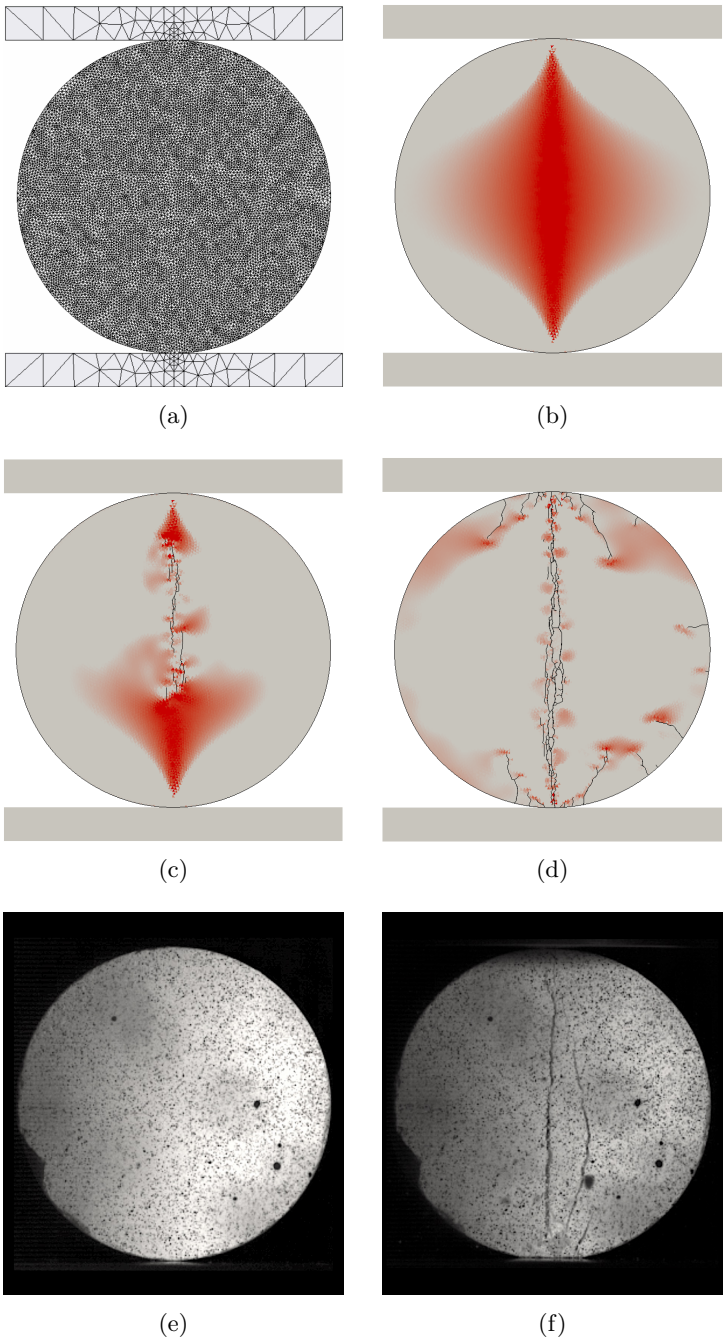

Figure 2: Simulation of the uniaxial compressive test on a cylinder without holes from Set 1: (a) triangular mesh discretisation of the specimen and loading plates. (b) Horizontal tensile stress field before failure reaching the value of tensile strength in the centre of the disc. (c) Crack propagating from the centre of the disc to the two sides and (d) splitting of the two sides of the disc and post failure fragmentation. Two frames from the video recording of the uniaxial compressive test on a cylinder without holes from Set 1: (e) before and (f) after failure.

for the weak orientations.

A mesh sensitivity analysis has been carried out for the uniaxial compression test simulations. The disc without holes from Set 1 has been discretised with four different realisations of a 150 μm element size mesh (Figure 8) obtained with three different values for the rigid rotation about the centre of the disc. With the same process, four different realisations of a 100 μm element size mesh have also been obtained, as shown in Figure 9. The load-displacement curves for the four realisations of a 150 μm element size mesh are shown in Figure 6. Figure 7 shows the load-

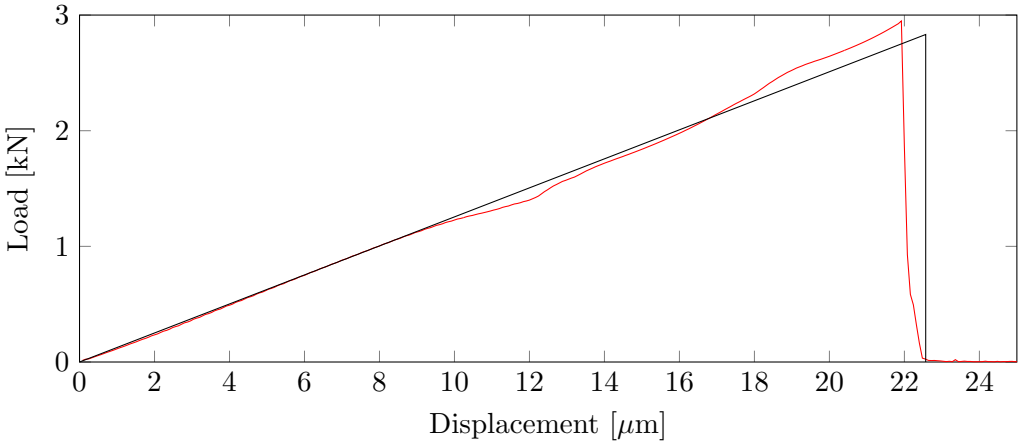

Figure 3: Load-displacement curve for the uniaxial compressive test on a cylinder without holes from Set 1: comparison between the numerical results (red) and the the approximated experimental curve (black) calculated with equation (1).

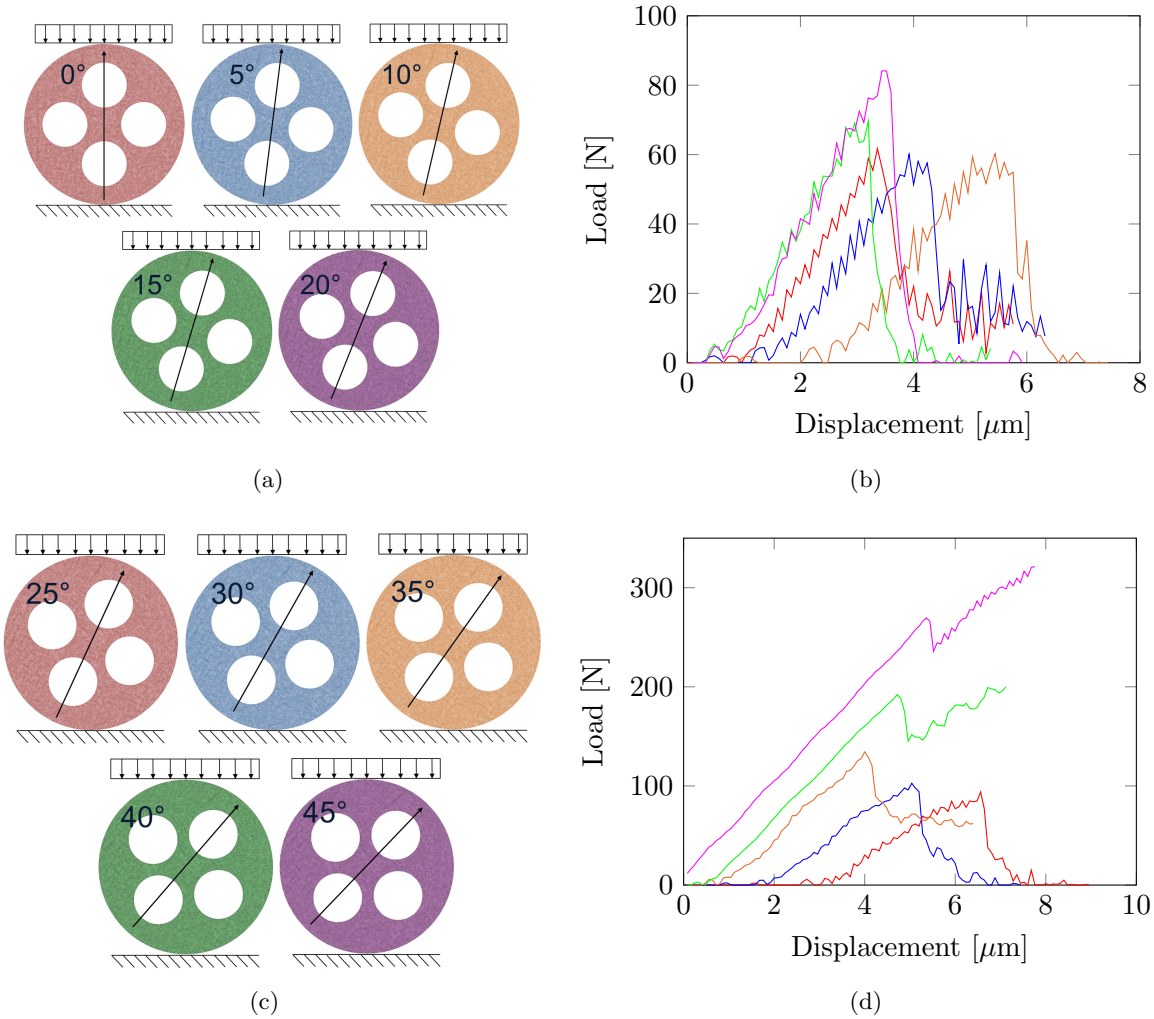

Figure 4: Boundary conditions and load-displacement curves obtained from uniaxial compressive test simulations on the four-hole specimens from Set 1 for orientation angles: (a,b) 0° (red), 5° (blue), 10° (orange), 15° (green), 20° (magenta) and (c,d) 25° (red), 30° (blue), 35° (orange), 40° (green) and 45° (magenta).

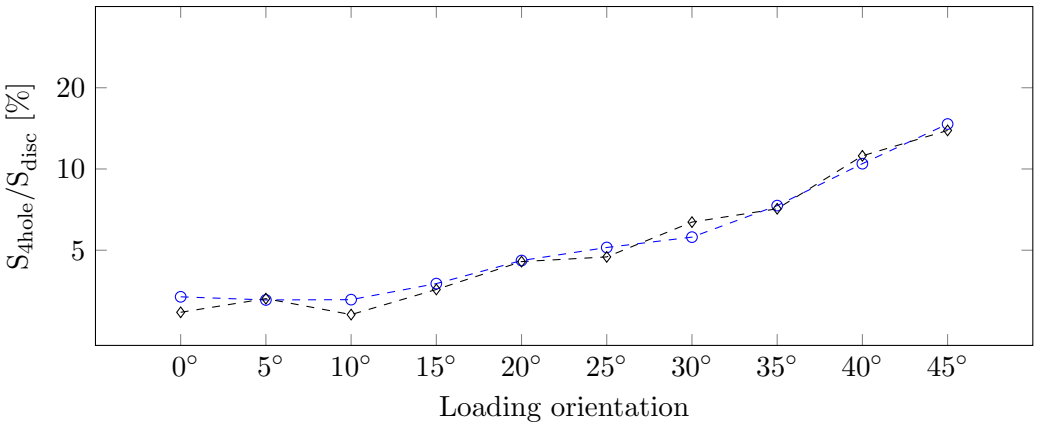

Figure 5: Relation between the loading orientation and the structural strength of four-hole pellets, normalised with respect to the strength of an equivalent cylinder without holes. Numerical results for Set 1 (blue) and Set 2 (black).

displacement curves for the four realisations of a 100 μm element size mesh. The initial part of the plots show the load take up with displacement is sensitive to the initial contact condition of the specimen with the two loading plates, which varies in due to the rigid rotation of the mesh. This causes small fluctuations in the load-displacement curves in Figure 7. The peak values of the load for the 8 realisations of the 150 μm and 100 μm element size are consistent with the theoretical peak load values also plotted in the figures, suggesting there are no significant unintended anisotropies in stiffness and strength imposed by the unstructured meshing tool employed.

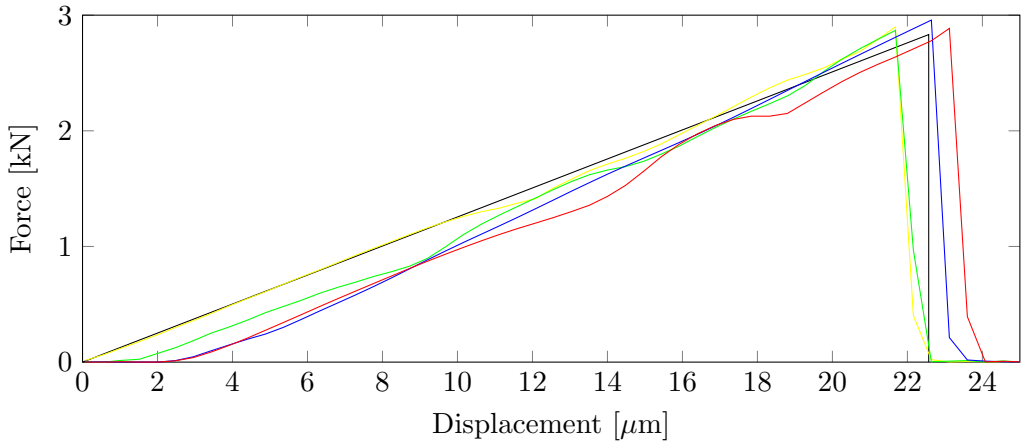

Figure 6: Mesh sensitivity analysis for the uniaxial compression test simulations: comparison of the load-displacement curve calculated in the numerical simulations for the 150 μm mesh obtained with 0° (yellow), 10° (green), 20° (blue) and 30° (red) rotation of the original mesh of the disc. The approximated experimental curve for Set 1 (black) is also plotted.

4 Conclusions

The numerical results of uniaxial compressive tests on cylinders without holes (Brazilian disc tests) have been presented. The contact force extrapolated from the numerical simulations has been compared to corresponding approximated experimental curves, giving further confirmations [3] of a correct simulation of mode I fracture in porous ceramic pellets. A mesh sensitivity analysis has also been carried out for the uniaxial compression test simulations, suggesting that there are no significant unintended anisotropies in stiffness and strength imposed by the unstruc-

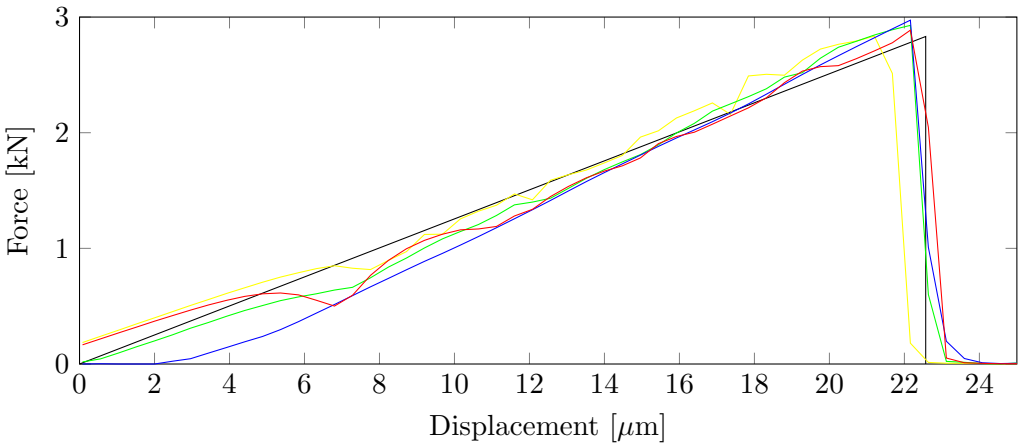

Figure 7: Mesh sensitivity analysis for the uniaxial compression test simulations: comparison of the load-displacement curve calculated in the numerical simulations for the 100 μm mesh obtained with 0° (yellow), 10° (green), 20° (blue) and 30° (red) rotation of the original mesh of the disc. The approximated experimental curve for Set 1 (black) is also plotted.

tured mesh employed in the FEMDEM simulations. The structural strength of complex-shaped pellets under simplified loading conditions was also investigated with numerical simulations. Loading orientations at intervals of 5° have been considered between the weak and the strong orientation configuration of the four-hole discs. The load at failure calculated in the numerical simulations for the different orientations of pellets from two sets of samples have been compared. The values of normalised load with respect to the strength of an equivalent cylinder of identical geometry and mechanical properties without holes have been shown to be in good agreement for two sets of samples with different sizes and mechanical properties. This provides a consistent relation between simplified loading conditions and the structural strength of four-hole discs, also giving an insight into the relation between the shape of catalyst supports and their mechanical performance. First confirmations of the Solidity FEMDEM code capabilities in representing realistic contact forces between complex-shaped catalyst pellets has been provided in previous works [6, 7]. Future research will be undertaken to compare the numerically inferred structural strengths with values obtained from real experiments on cylindrical pellets with four holes and to investigate other shape related catalyst performance properties, such as fragment size distributions of crushed pellets.

ACKNOWLEDGEMENTS

This research has been sponsored by the Engineering and Physical Sciences Research Council (EPSRC) and the Johnson Matthey Technology Centre.

REFERENCES

[1] J. R. Rostrup-Nielsen and T. Rostrup-Nielsen, "Large-scale hydrogen production," *CATTECH*, vol. 6, no. 4, pp. 150–159, 2002.

[2] Applied Modelling and Computation Group (AMCG) at Imperial College London, "Solidity FEMDEM code," *www.solidityproject.com*.

[3] A. Farsi, J. Xiang, J. P. Latham, A. D. Pullen, M. Carlsson, E. H. Stitt, and M. Marigo, "An application of the finite-discrete element method in the simulation of ceramic breakage: methodology for a validation study for alumina specimens," in *IV International Conference on Particle-based Methods Fundamentals and Applications PARTICLES 2015*, no. November, pp. 1–12, 2015.

[4] Q. Z. Wang, X. M. Jia, S. Q. Kou, Z. X. Zhang, and P. a. Lindqvist, "The flattened Brazilian disc specimen used for testing elastic modulus, tensile strength and fracture toughness of brittle rocks: Analytical and numerical results," *International Journal of Rock Mechanics and Mining Sciences*, vol. 41, no. 2, pp. 245–253, 2004.

[5] A. Munjiza, *The Combined Finite-Discrete Element Method*. Wiley, 2004.

[6] A. Farsi, J. Xiang, J.-P. Latham, M. Carlsson, E. H. Stitt, and M. Marigo, *Simulation and Characterisation of Packed Columns for Cylindrical Catalyst Supports and Other Complex-Shaped Bodies*, pp. 397–406. Singapore: Springer Singapore, 2017.

[7] J. Xiang, J. Latham, and A. Farsi, *Algorithms and Capabilities of Solidity to Simulate Interactions and Packing of Complex Shapes*, pp. 139–149. Singapore: Springer Singapore, 2017.

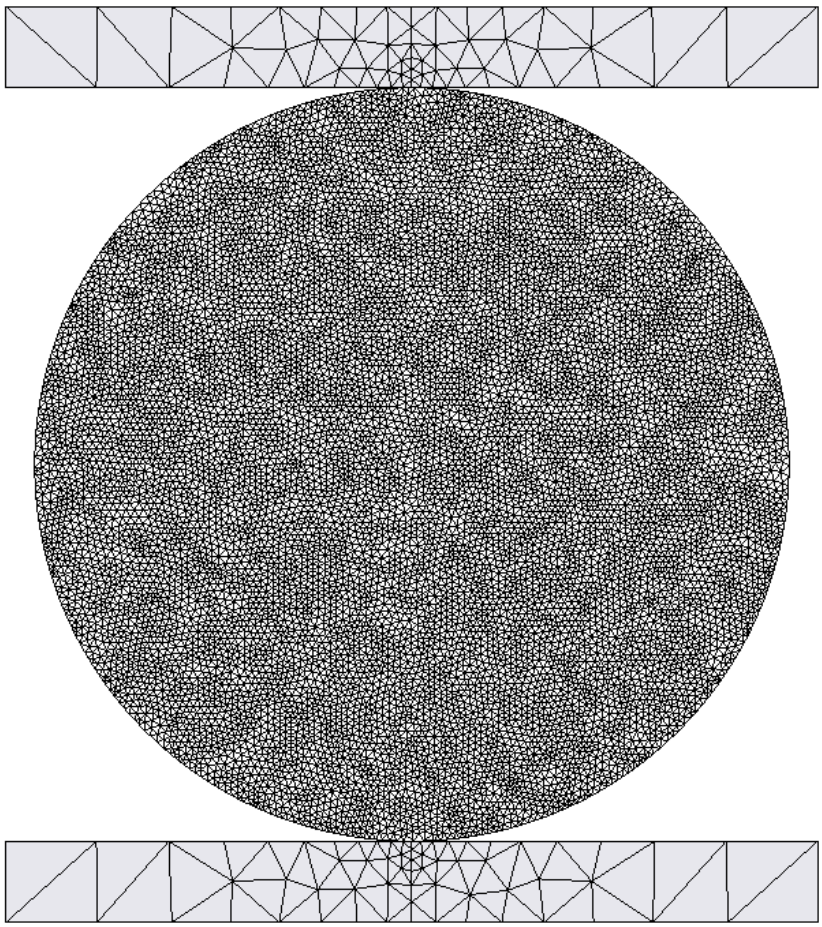

Figure 8: Mesh sensitivity analysis for the uniaxial compression test simulations: triangular mesh discretisation of the test setup for the 150 μm mesh. The mesh is then rotated of 10°, 20° and 30° to preform a comparison of four different mesh realisations with the same element size.

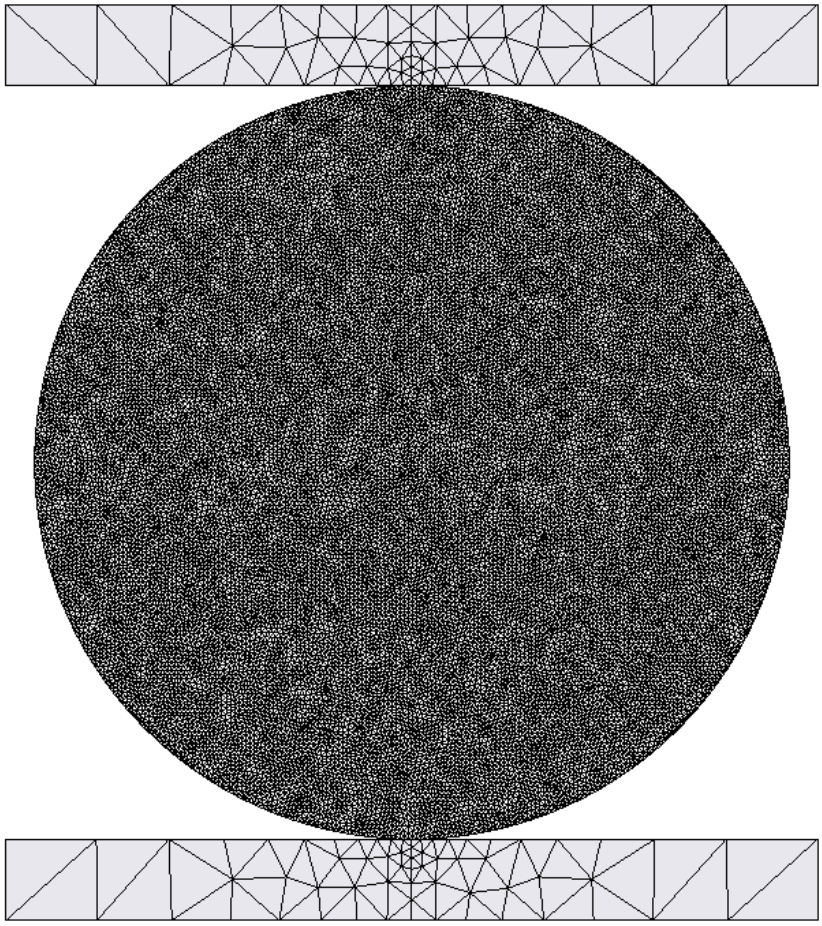

Figure 9: Mesh sensitivity analysis for the uniaxial compression test simulations: triangular mesh discretisation of the test setup for the 100 μm mesh. The mesh is then rotated of 10°, 20° and 30° to preform a comparison of four different mesh realisations with the same element size.